

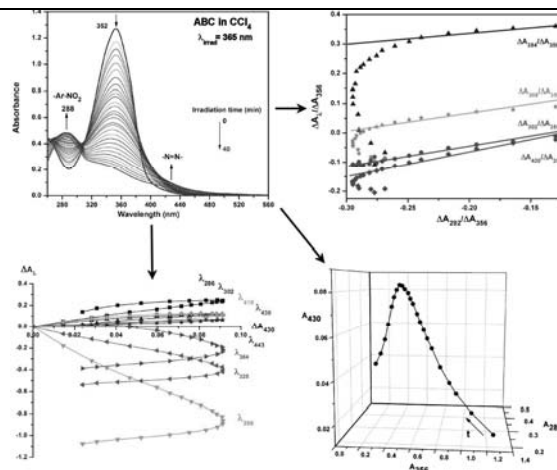
## PHOTOCHEMICAL REACTIONS OF 2,6-DI(4'-AZIDOBENZYLIDENE)-METHYLCYCLOHEXANONE IN FLUID MEDIA\*\*

Mihaela AVADANEI\*

\*"P. Poni" Institute of Macromolecular Chemistry, 41A Grigore Ghica Voda Alley, 700487 Iași, Roumania

Received March 7, 2016

Photolysis of 2,6-di(4'-azidobenzylidene)-methylcyclohexanone was performed in a series of solvents under 365 nm radiation, in the presence or absence of two polymers, and was monitored by UV-Vis spectroscopy. The spectral analysis revealed that the photochemistry of this bisazide involved at least three consecutive photoreactions in most cases. The photogenerated species, largely recognized as amino, nitro and azo species, are unstable and have undergone further decomposition. The most interesting photolysis is seen in the methanol solution, from both spectral and mechanistic point of views. Based on the UV-Vis spectral changes, the photoreactions course in methanol solution has been sketched.



### INTRODUCTION

Photolysis of aryl azides is still one of the most investigated reactions, because the chemistry of the photogenerated nitrene radicals is particularly rich and has large implication in the practical applications and chemistry fundamentals. Besides the expected sensitivity to the substitution to the aromatic ring, the nature, the spin state and lifetime of the intermediates are extremely sensitive to several medium factors. The nitrene chemistry can be directed into specific reaction channels by a proper selection of the chemical reactivity of the substrate, temperature and viscosity of the medium,<sup>1-3</sup> light intensity<sup>4,5</sup> or wavelength,<sup>6</sup>

presence of oxygen<sup>7</sup> and azide concentration.<sup>4</sup> At high azide amounts or high intensity of the radiation source,<sup>8</sup> the self-coupling reactions with formation of azo – derivatives or polymeric products are preferred, but these compounds are often seen as by-products. In substrates that are potentially donors of hydrogen atoms, the formation of anilino or primary amine terminal groups dominates, which can be given by the nitrene reacting in either singlet or triplet state.

The large use of aryl azides in the photocrosslinking of synthetic,<sup>7-15</sup> natural,<sup>16</sup> or biological systems<sup>17-19</sup> is mainly based on the insertion of the singlet nitrene into CH, NH or OH bonds or, in a lesser extent, by linking through azo

\* Corresponding author: mavadanei@icmpp.ro.

\*\* Supporting Information on <http://web.icf.ro/rrch/> or <http://revroum.lew.ro/>

bonds. In the particular case of bis-azides, the two reactive units might photolyse one at the time and the corresponding photoactivated bis-azide can further react with only one nitrene radical. This situation has been observed when a very used photoinitiator, 2,6-di(4'-azidobenzylidene)-methylcyclohexanone that is known as ABC diazide, has been photolysed in the presence of 3-methyl-1-butene in a benzene solution.<sup>20</sup> The main reactions of the photogenerated nitrenes has been found to be the attack to the  $\pi$  system of the C=C bonds, the insertion into CH bonds and the hydrogen abstraction, all of these leading to aziridine rings and secondary and primary amine groups.<sup>20</sup> No ring-expansion products, such as keteneimine structures, nor polymeric tar were detected. In addition, a quite large amount of azo-derivatives has been isolated. These reactions have been used to make clear the photocrosslinking mechanism of 1,2-polybutadiene initiated by 2,6-di(4'-azidobenzylidene)-methylcyclohexanone.

The conclusions from this study<sup>20</sup> are in agreement to the vast amount of studies concerning the photochemistry of aryl azides, the complexity of their photoreactions coming from the fact that the intermediates can take several forms and the reaction mixture consists of many species. However, the extreme high reactivity of ABC is a double-edged sword, because the quick response of ABC to UV light and efficient crosslinking process is counterbalanced by the fact that the nitrenes can be engaged in several reactions that do not conduct to the polymer crosslinking, so that their main purpose can be lost. Starting from the identified photoproducts of the ABC photolysis in solid state, when it has been used as a photoinitiator in the crosslinking of elastomers,<sup>20</sup> the study of the ABC photochemistry continued by following its photolysis in other solid and fluid media. A part of the investigation in solid media has been performed as a comparative analysis between its reactions in the soft 1,2-polybutadiene (1,2-PB) and rigid poly(methyl methacrylate) matrix (PMMA).<sup>20</sup> In the present study, the photochemistry of ABC has been extended to fluid solutions, at first following the photocrosslinking mechanism in a less viscous medium.

The results in this manuscript are presented as a spectral and spectrokinetic analysis of ABC photolysis in several solvents, which are differentiated by the presence or lack of labile hydrogen atoms. More specific, ABC has been irradiated with soft UV light (365 nm) in: (a) two ternary systems: ABC – 1,2-PB in a CHCl<sub>3</sub>

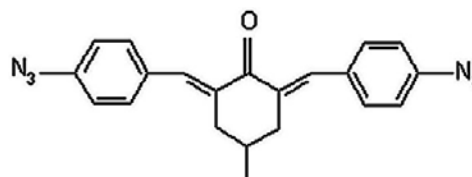
solution, and ABC – PMMA in a CHCl<sub>3</sub> solution; (b) in CCl<sub>4</sub>, CHCl<sub>3</sub> and CH<sub>3</sub>OH. With the aid of absorbance difference (AD) and absorbance difference quotients diagrams (ADQ), and also of the 3D-plots in the Mauser space,<sup>21-23</sup> the spectroscopic features specific to every type of photoreactions undergone by ABC in each case were analyzed.

## MATERIALS AND METHODS

**Materials.** 2,6-di(4'-azidobenzylidene)-methylcyclohexanone (ABC, Sigma - Aldrich) was used as received. 1,2-Polybutadiene (1,2-PB) (Japan Synthetic Rubber Company) have 92% 1,2-unit content, with a predominant syndiotactic microstructure,  $M_w$  of 92 000 g/mol and  $M_w/M_n = 1.75$ ,  $T_g = -20$  °C,  $T_m = 80$  °C (DSC data), and crystallinity of 25%. Poly(methyl methacrylate) (PMMA, Sigma - Aldrich) has  $M_w = 120000$  and  $T_g = 105$ °C. The solvents CCl<sub>4</sub> (analytical grade, Aldrich), CHCl<sub>3</sub> (spectroscopic grade, Aldrich) and MeOH (spectroscopic grade, Fluka) were used as received. Scheme 1 presents the chemical structure of ABC.

**Sample preparation.** Solutions of  $4.5 \times 10^{-5}$  mol/L of ABC in the cited solvents, introduced in a quartz cell of 10 mm optical path (3 mL) were irradiated by the 365 nm line of a 350 W medium pressure mercury lamp (LOS-2, Russian Federation). For the photolysis of ABC in the presence of polymer, the concentration of azide was  $3.8 \times 10^{-6}$  mol/L.

**Irradiation and spectral measurements.** The photoreactions were monitored by means of UV-Vis spectroscopy, with a Specord M-200 UV-Vis spectrometer. The spectra were recorded at specific time intervals. The measured radiation intensity was 7 W/m<sup>2</sup>, corresponding to an irradiance of  $2.1 \times 10^{-9}$  Einstein cm<sup>-2</sup> s<sup>-1</sup>. The irradiation times were prolonged to a photostationary state. Before irradiation, the oxygen has been removed by bubbling the solutions with argon gas. The spectral analysis showed that this procedure still did not completely remove the solvated oxygen.



Scheme 1 – Chemical structure of 2,6-di(4'-azidobenzylidene)-methylcyclohexanone (ABC).

## RESULTS AND DISCUSSION

### 1. Photoreactions of ABC with 1,2-PB and PMMA in a $\text{CHCl}_3$ solution

Interaction of aryl nitrenes derived from ABC with different substrates in fluid media has been at first evaluated by studying the ABC photoreactions with 1,2-PB and PMMA in a  $\text{CHCl}_3$  solution. In a previous study, irradiation of ABC in 1,2-PB and PMMA in solid state led to photocrosslinking of 1,2-PB, as expected, and with no serious differences in the overall quantum yield of the azido group transformation.<sup>20</sup> The main photoreactions of ABC with 1,2-PB were the hydrogen abstraction from the allylic group and the attack of nitrenes to the  $\text{C}=\text{C}$  bonds. On the other side, the hydrogen abstraction from PMMA can take place only from the methine group and this was indeed observed, by the formation of amine moieties. Generation of the amino groups was

found to be faster in a PMMA film, because the rigidity of the matrix hindered the free movement of the monoanilino radicals far away from their generation site. In turn, the formation of azo compounds was taking place with similar rate constants and it resulted that the PMMA rigidity has no influence on it. Therefore, changing the physical state of the matrix has been thought to influence the rate constants of the main photoreactions.

At first, photoreactions of ABC with 1,2-PB and PMMA in a liquid formulation, using  $\text{CHCl}_3$  as a solvent, have been performed. As follows from Figs. 1 and 2, two distinct aspects were observed as regarding the time-dependent spectral changes: (i) the ABC photolysis proceeded more uniformly in 1,2-PB, where the two isobestic points have been preserved near the end, and (ii) the amount of the azo dimers increased in the PMMA solution and decreased in that of 1,2-PB, as compared to those in films.

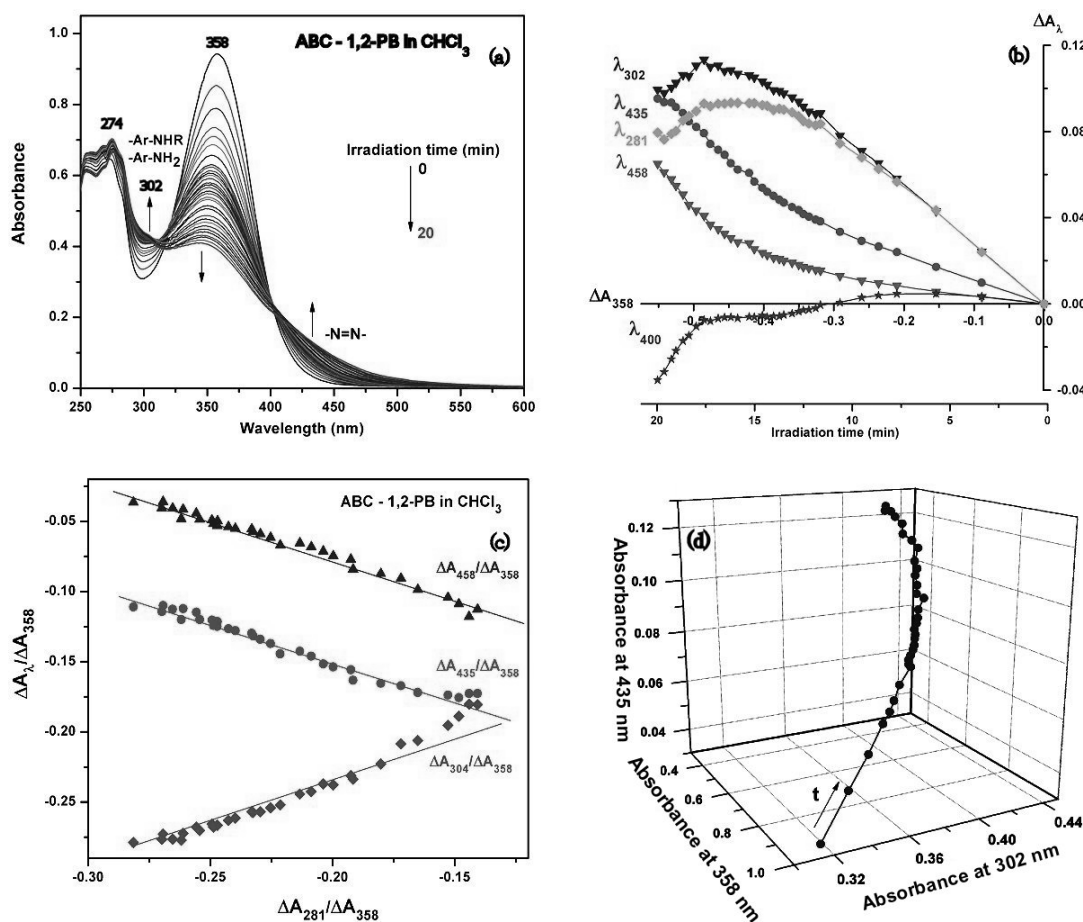


Fig. 1 – Spectral analysis of the ABC bisazide photoreactions with 1,2-PB in a  $\text{CHCl}_3$  solution: (a) temporal changes of the UV-Vis spectra; (b) linear absorbance difference diagram (AD-diagram) as a function of the central maximum of the azide absorption; (c) the absorbance quotient diagram (ADQ diagram); (d)  $A_{358}$  vs.  $A_{302}$  vs.  $A_{435}$  diagram. The wavelength of 400 nm is corresponding to the isobestic point.

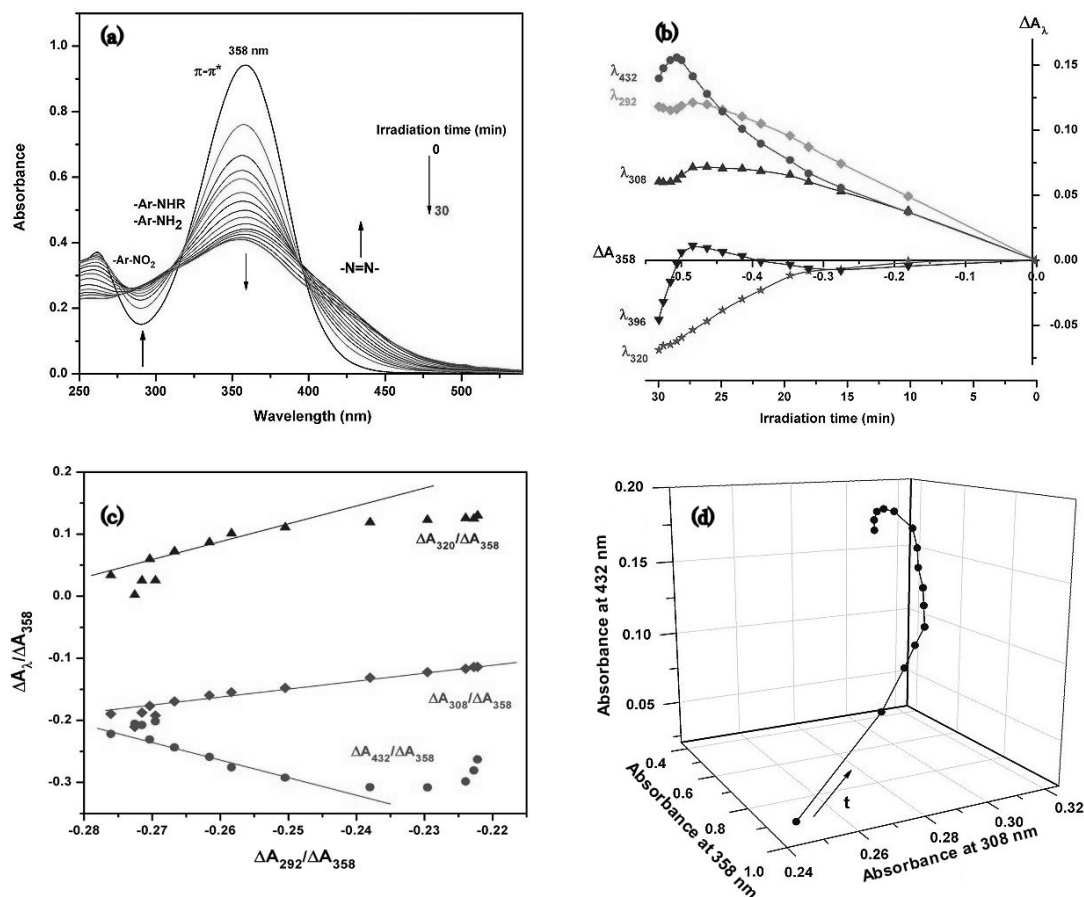


Fig. 2 – ABC photolysis in the presence of PMMA in a  $\text{CHCl}_3$  solution: (a) temporal changes of the UV-Vis spectra; (b) linear absorbance difference diagram (AD-diagram) as a function of the central maximum of the azide absorption; (c) the absorbance quotient diagram (ADQ diagram); (d)  $A_{358}$  vs.  $A_{308}$  vs.  $A_{432}$  diagram. The wavelength of 396 nm is corresponding to the isosbestic point.

The spectroscopic analysis presented in Fig. 1 shows that the photolysis of ABC in a  $\text{CHCl}_3$  solution of 1,2-PB resulted in an different development of the photogenerated groups as compared to that in film. One can see the quite uniform evolution of the azo groups (435 nm) (Fig. 1 (b)) and the curvature in those of the nitro (302 nm) and amines (281 nm), simultaneously with the loss of the isosbestic point at 400 nm after a certain period of time. The AD diagram evaluated at the wavelength of the nitro or amine band, (not shown) is characteristic to two photo-consecutive reactions. The ADQ diagram for the evolution of amine absorption band loses its linearity in the second part of the irradiation period, giving a proof for the existence of more than two independent reactions (Fig. 1 (c)): formation of amine groups and their conversion into another chemical species, yet to be identified. The 3D Mauser space illustrated in Fig. 1 (d) is showing the relationship between the intensities of the 358, 302 and 435 nm bands. It can be seen that the dimerization reactions accelerated once a certain amount of

nitro (or amine) groups has been reached. The two consecutive photoreactions maintained their evolution till the last  $\approx 5$  min of irradiation. From here, the 3D plot lays no more in a plane and another consecutive reaction(s) occurred.

Similar characteristics of consecutive reactions are observed in the AD-diagrams of the ABC photolysis in the presence of PMMA, in the  $\text{CHCl}_3$  solution (Fig. 2). The AD-diagram evaluated at the initial ABC maximum (358 nm) shows the bent data curves for all the photogenerated chemical groups (Fig. 2 (b)). The curvature in the ADQ diagrams also indicate the occurrence of the third consecutive reaction in which the azo groups are involved (Fig. 2 (c)). It thus appears that the photoreactions became more complicated in the last minutes of irradiation, made it certain by the intricate shape of the  $A_{358}$  vs.  $A_{308}$  vs.  $A_{432}$  3D-plot (Fig. 2 (d)). As a partial conclusion, the decomposition of the nitro and amine groups under prolonged irradiation parallels the continuous decay of the azide groups and the building up of the azo derivatives.

Table 1

The kinetic parameters and the overall quantum yield for the azide consumption in the ABC bisazide photolysis in the presence of 1,2-PB or PMMA

Substrate	$k_{\text{nitro/nitroso}}$ ( $\times 10^{-2} \text{ s}^{-1}$ )	$k_{\text{amine}}$ ( $\times 10^{-2} \text{ s}^{-1}$ )	$k_{\text{azides } \pi-\pi^*}$ ( $\times 10^{-2} \text{ s}^{-1}$ )	$k_{\text{azo}}$ ( $\times 10^{-2} \text{ s}^{-1}$ )	$\phi_{356}^*$
1,2-PB in $\text{CHCl}_3$	9.07	10.12	6.166	5.10	0.38
PMMA in $\text{CHCl}_3$	9.86	28.54	8.75	4.10	0.74
1,2-PB*	9.31	10.103	9.67	7.61	0.411
PMMA*	3.18	23.6	6.36	9.94	0.422

\*-taken from Ref. [20].

The decrease of azide absorbance with the irradiation time is of first order only in the first minutes of exposure. A linear fit of the equation  $\ln[(A_0 - A_\infty)/(A_t - A_\infty)] = k \cdot t$  made for the linear part of the plots gave the rate constants of the azide photolysis and of the photoproducts generation that are listed in Table 1.  $A_0$ ,  $A_t$  and  $A_\infty$  are the initial absorbance, at a time  $t$ , and in photostationary state, respectively. When compared to the irradiation in solid state, the azide decomposition started faster in PMMA, in both liquid and solid media, and its consumption is higher when photolyzed in solution. The same classification results for the amino or azo group generation, because the development of amines in PMMA occurs twice as fast ( $k_{\text{amine}} = 28.54 \times 10^{-2} \text{ s}^{-1}$ ) as in PB ( $k_{\text{amine}} = 10.1 \times 10^{-2} \text{ s}^{-1}$ ), in solid film or  $\text{CHCl}_3$  solution. The similar values of  $k_{\text{amine}}$  for the 1,2-PB substrate in solution and film might exclude the idea that the hydrogen abstraction by the aryl nitrenes from  $\text{CHCl}_3$  would supplement that from the polymer. In the PMMA –  $\text{CHCl}_3$  system, it appears that the hydrogen abstraction took place from both the solvent and PMMA.

## 2. Exploring the ABC photolysis in several solvents

Next, the ABC photolysis has been studied in several liquid media, differentiated by the site for hydrogen abstraction, that is  $\text{CHC}_3\text{OH}$  and  $\text{CHCl}_3$ , and also in the inert  $\text{CCl}_4$ . The characteristic absorption band of the  $\pi-\pi^*$  transition decreased more slowly as the substrate has a higher ability to donate a hydrogen atom. The electronic absorption spectra collected in Figs. 3 (a), 4 (a) and 5 (a) show the almost complete consumption of azide in  $\text{CCl}_4$  after 40 min of irradiation (conversion of  $\approx 86\%$ ) and the less than half-

photolyzed ABC ( $\approx 32\%$ ) in  $\text{CHC}_3\text{OH}$ , after 60 min. Two broad absorption bands developed during irradiation and the final spectra have the maxima around 300 and 430 nm, with the residual azide absorption around 360 nm. In  $\text{CH}_3\text{OH}$  solution, the visible maximum is red-shifted and is centered on 455 nm. As expected, the amounts of nitro (and maybe nitroso), amine and azo groups vary according to the location of the labile hydrogen in the substrate. In  $\text{CCl}_4$  solution, the lack of a labile hydrogen atom conducts the nitrenes in their singlet state to the interaction with the residual molecular oxygen giving rise to the nitro moieties ( $\lambda_{\text{abs}} \approx 290 \text{ nm}$ ), while the triplet nitrenes may form nitroso groups or led to the formation of azo-dimers. The isosbestic point around 400 nm in the spectra recorded in potentially donors of hydrogen atoms, such as  $\text{CH}_3\text{OH}$  and  $\text{CHCl}_3$ , indicate that the azo-compounds are the only photoproduct with absorption in this area. In addition, the azo and amine bands are highest in  $\text{CHC}_3\text{OH}$ , but are in contradiction with the still high intensity of the azide maximum.

The reaction rates and the overall quantum yield of azide conversion, listed in Table 2, got lower as the dielectric constant of the solvent was higher. The exception is made by the reaction of nitrenes with the residual molecular oxygen to give nitro/nitroso groups. The rate constant of the azide group photolysis decreased with one order of magnitude from  $\text{CCl}_4$  ( $7.73 \times 10^{-2} \text{ s}^{-1}$ ) to  $\text{CHC}_3\text{OH}$  ( $7.04 \times 10^{-3} \text{ s}^{-1}$ ), while the quantum yield decreased more than five times. With the exception of the development of the azo derivatives, the initial rate for apparition of the nitro/nitroso and amine terminal groups is of the same order of magnitude irrespective the substrate.

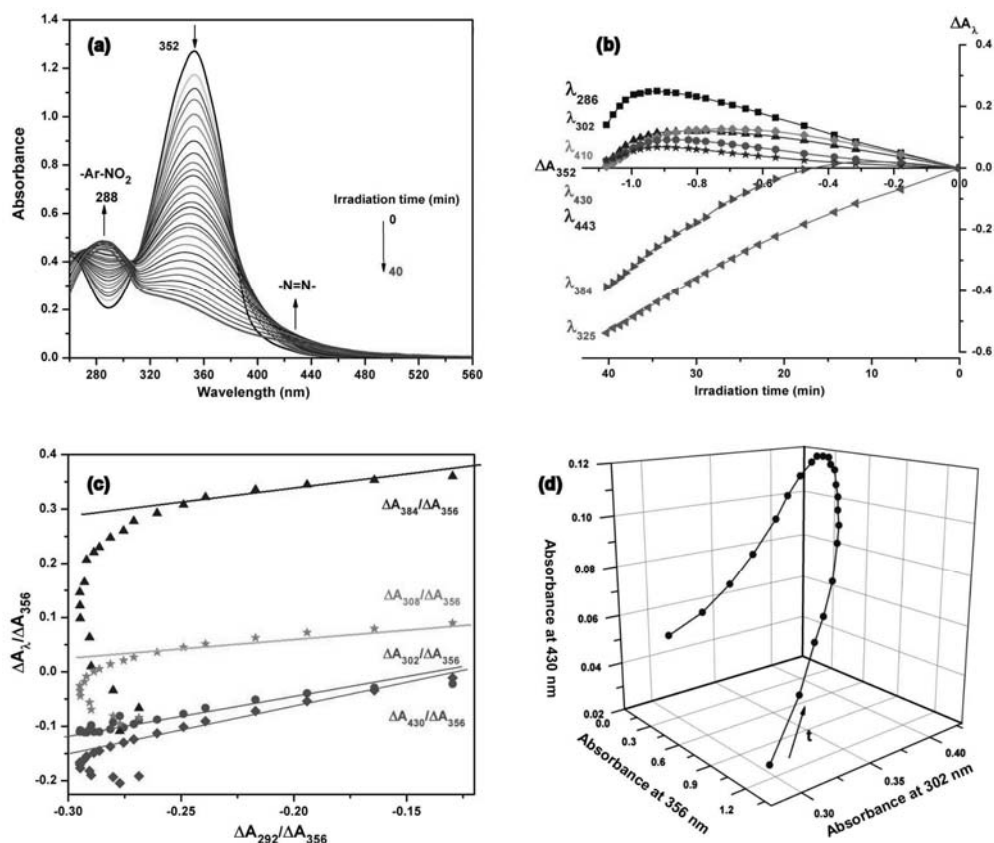


Fig. 3 – Spectral analysis of the ABC photolysis ( $\lambda_{\text{irrad}} = 365 \text{ nm}$ ) in  $\text{CCl}_4$  from several perspectives: (a) temporal changes of the UV-Vis spectra; (b) linear absorbance difference diagram (AD-diagram) with several monitored wavelengths; (c) the absorbance quotient diagram (ADQ diagram); (d) the  $A_{356}$  vs.  $A_{286}$  vs.  $A_{430}$  diagram.

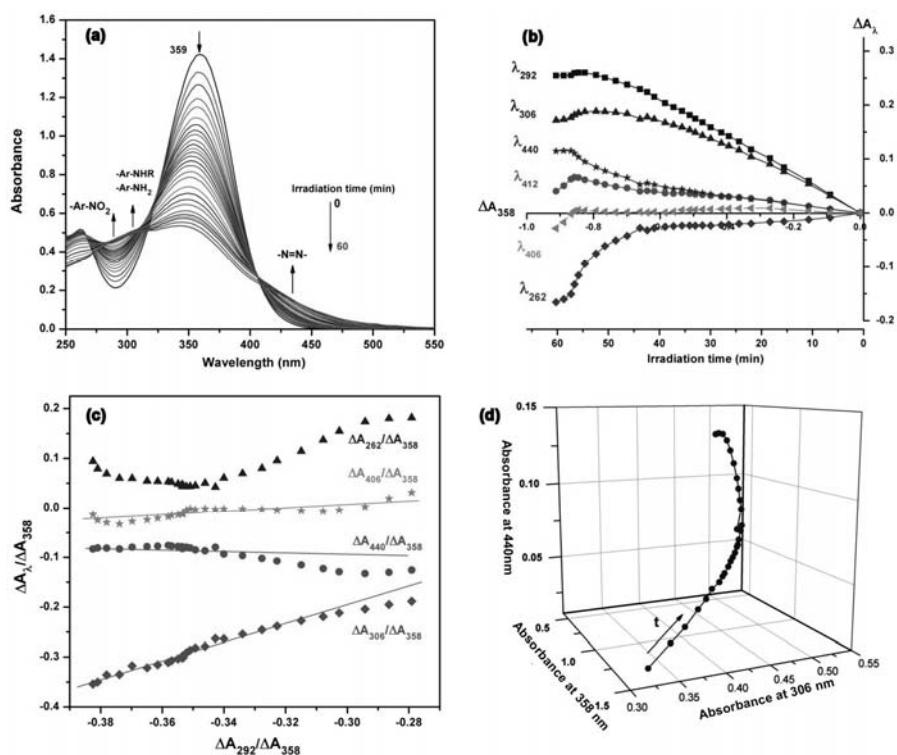


Fig. 4 – Spectral analysis of the ABC photolysis ( $\lambda_{\text{irrad}} = 365 \text{ nm}$ ) in  $\text{CHCl}_3$ : (a) temporal changes of the UV-Vis spectra; (b) linear absorbance difference diagram (AD-diagram) with several monitored wavelengths; (c) the absorbance quotient diagram (ADQ diagram); (d) the  $A_{358}$  vs.  $A_{306}$  vs.  $A_{440}$  diagram. The wavelength of 406 nm is corresponding to the isosbestic point.

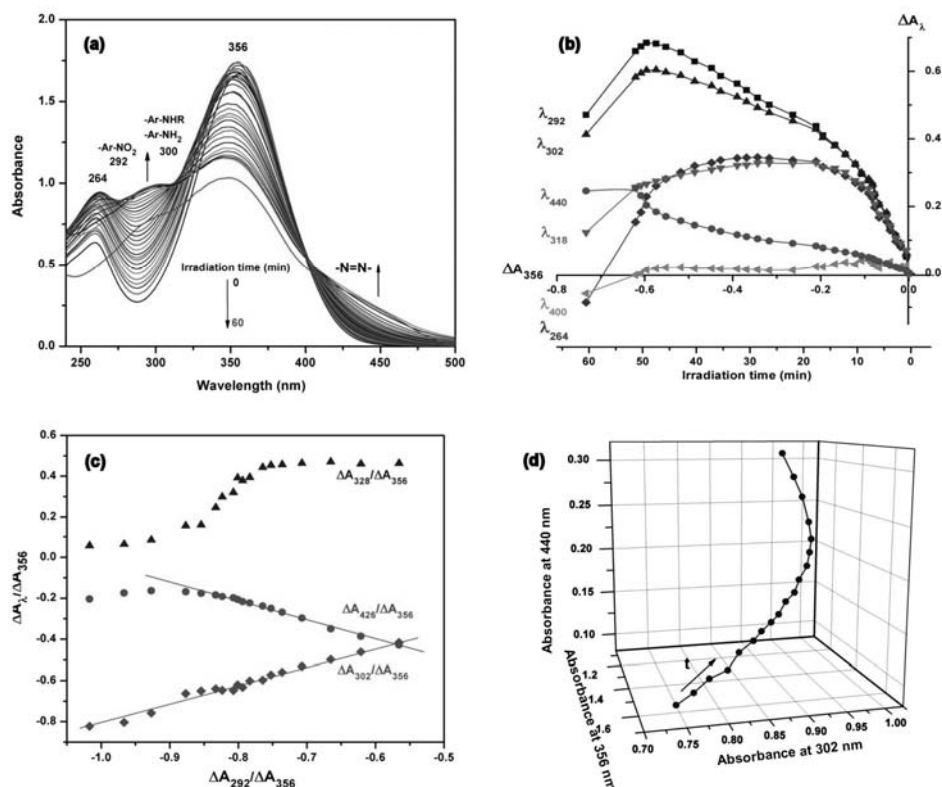


Fig. 5 – Spectral analysis of the ABC photolysis ( $\lambda_{\text{irrad}} = 365 \text{ nm}$ ) in  $\text{CH}_3\text{OH}$ : (a) variations of the UV-Vis spectra; (b) linear absorbance difference diagram (AD-diagram) with several monitored wavelengths; (c) the absorbance quotient diagram (ADQ diagram); (d) the  $A_{356}$  vs.  $A_{302}$  vs.  $A_{440}$  diagram. The wavelength of 400 nm is corresponding to the isosbestic point.

Table 2

The kinetic parameters and the overall quantum yield for the azide consumption in the ABC bisazide photolysis in  $\text{CCl}_4$ ,  $\text{CHCl}_3$  and  $\text{CH}_3\text{OH}$

Substrate	$k_{\text{nitro/nitroso}}$ ( $\times 10^{-2} \text{ s}^{-1}$ )	$k_{\text{amine}}$ ( $\times 10^{-2} \text{ s}^{-1}$ )	$k_{\text{azides } \pi-\pi^*}$ ( $\times 10^{-2} \text{ s}^{-1}$ )	$k_{\text{azo}}$ ( $\times 10^{-2} \text{ s}^{-1}$ )	$\phi_{356}^*$
$\text{CH}_3\text{OH}$	1.06	2.83	0.704	0.43	0.16
$\text{CHCl}_3$	8.01	11.37	5.40	3.36	0.52
$\text{CCl}_4$	7.42	12.1	7.73	7.68	0.87

The AD-diagram traced at the central maximum wavelength (Fig. 3 (b), Fig. 4 (b) and Fig. 5 (b)) shows that the most uniform photodecomposition of ABC is observed in  $\text{CHCl}_3$ , while in  $\text{CH}_3\text{OH}$  it occurred in several stages. The plots are straight lines for the most of the irradiation period in  $\text{CCl}_4$  and  $\text{CHCl}_3$  and are strongly distorted in the  $\text{CH}_3\text{OH}$  solution, excepting the data corresponding to the azo groups. The negative slopes obtained for some of the monitored wavelengths suggest that several of the photoproducts absorb at those wavelengths. Finally, it appears that the long irradiation times led to destruction of almost all types of photoproducts, irrespective of the substrate.

The ADQ-diagrams show bent curves for irradiation in  $\text{CCl}_4$  (Fig. 3 (c)) and strong

deviations from linearity for irradiation in  $\text{CHCl}_3$  (Fig. 4 (c)) and  $\text{CH}_3\text{OH}$  (Fig. 5 (c)). Involvement of at least three consecutive reactions seems to be a common feature for the ABC photolysis in these solvents.

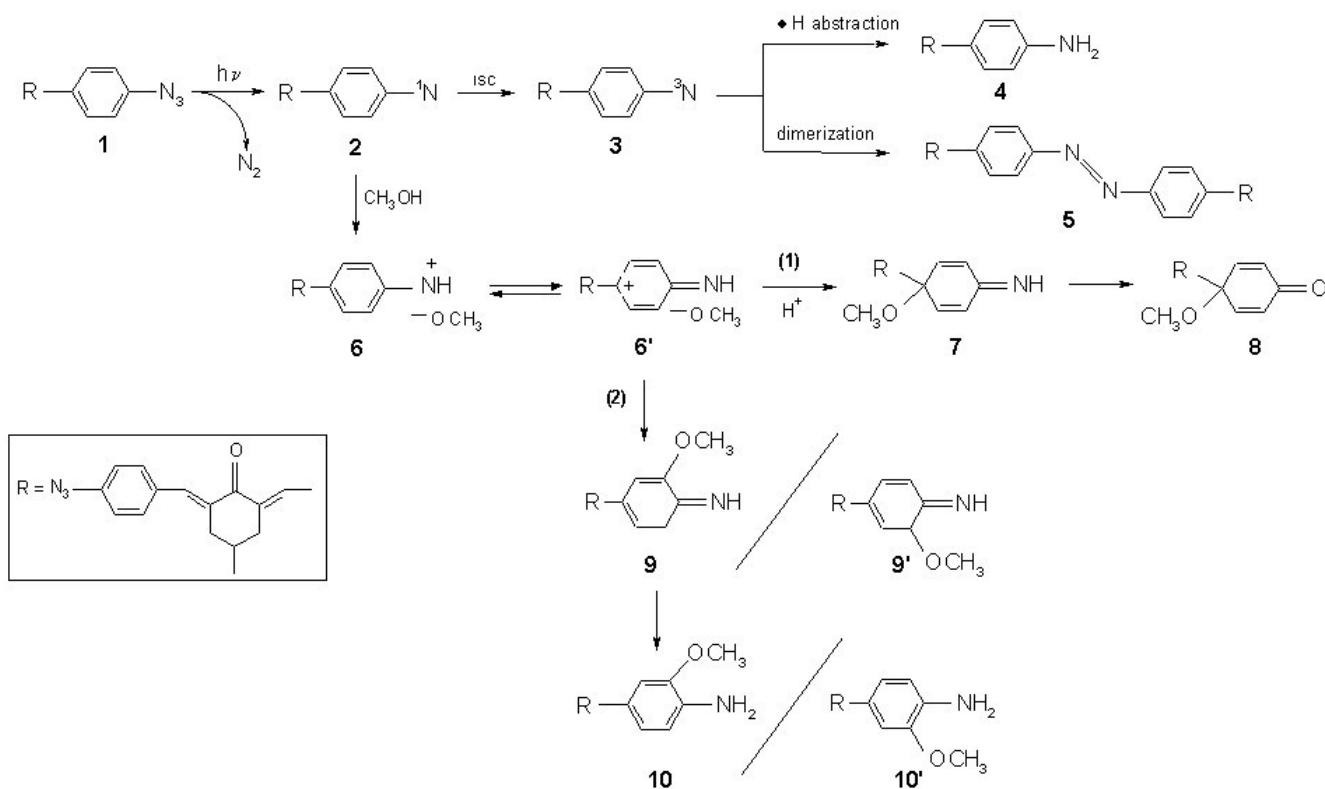
The graphical representation in the 3D Mauser space shows how the relationship between the initial and final components is changing as a function of the chemical reactivity of the substrate. The existence of several independent reactions can be checked by various wavelength combinations. Figs. 3 (d), 4 (d) and 5 (d) illustrate the three-dimensional A diagrams with the azo group absorption as the z axis. Despite the looking – alike AD-diagrams, the 3D-plots of  $\text{CCl}_4$  and  $\text{CHCl}_3$  solutions are very different. In  $\text{CCl}_4$ , the diagram  $A_{356}$  vs.  $A_{286}$  vs.  $A_{430}$  (Fig. 3 (d)) is slightly

distorted and is not lying on a plane, suggesting the occurrence of some side processes, beyond the supposed recombination and photooxidation reactions. In  $\text{CHCl}_3$  (Fig. 4 (d)) and  $\text{CH}_3\text{OH}$  (Fig. 5 (d)), the curves are intriguingly similar and show a linear relationship, which might be put in agreement with the presence of the isosbestic point around 400 nm.

The spectral temporal changes and the new intense and red-shifted visible absorption suggest that the methanolic chemistry of ABC upon UV irradiation is particularly complex and it can be analyzed in terms of photoreactions of azides in protic solvents. The photolysed ABC gave no noticeable polymeric tar in any of the solvents and neither when irradiated in the presence of 3-methyl-1-butene in a benzene solution.<sup>20</sup> These data indicate the lack of dihydroazepines as intermediates<sup>25</sup> and thus disregarding the ring expansion as one of the reaction channels. All these typical processes of the singlet and triplet nitrenes are generally occurring in aprotic solvents. In the protic methanol, the singlet nitrene can react with the solvent molecules in two different ways. The first one would be the insertion of the singlet nitrene into the OH bond of the alcohol, leading to a hydroxylamine ether. The second one is the

protonation of the singlet nitrene, readily taking place in aqueous, alcoholic,<sup>26-29</sup> or acidic solutions media.<sup>27,30</sup> In this particular case, the reaction rate must be higher than the other reaction channels, namely insertion reaction into the CH or OH bonds of the substrate and intersystem crossing to the triplet state. The arylnitrenium ion thus formed is usually stabilized by electron – donating groups in the *para* position.<sup>30-32</sup>

In the ABC photolysis in  $\text{CH}_3\text{OH}$ , the resulted bis(4-methylcyclohexanone-phenylnitrenium) ion, or, as previous irradiation studies showed that ABC photolyses at only one azide end,<sup>20</sup> the monophenylnitrenium ion, can be trapped by the methanol molecules. The nucleophilic addition of methanol can take place at either the *ortho* or *para* carbons of the aromatic ring<sup>31-33</sup> or to the *meta* position in some cases.<sup>34</sup> A second pathway would be the reduction of the bis(4-methylcyclohexanone-phenylnitrenium) ions to a final amine structure, by a sequential H atom abstraction. Taking into account these processes and the spectral changes, Scheme 2 summarizes the probable intermediates, the final products and the corresponding reaction channels of the ABC photoreactions in  $\text{CH}_3\text{OH}$ .



Scheme 2 – Photoreactions of ABC bisazide likely to occur upon photolysis in methanol solution.



Protonation of the singlet bis(4-methylcyclohexanone-phenylnitrene) **2** results in the contact ion pair **6**, whose bis(4-methylcyclohexanone-phenylnitrenium) ion have the resonance structure **6'**. The unstable nucleophilic adducts **7**, **8** and **9** would rearrange into the final products **10**, **11** and **12**. The compounds **10** and **11** have an 4-amino-2-methoxyphenyl or 4-amino-5-methoxyphenyl moiety, while **12** might be produced through an unimolecular rearrangement. The parent amine **4** in reaction (2) is the reduction product of **6'**. The nucleophilic adducts of some mono-azides such as 4-amino-3-nitrophenyl azide have a calculated absorption band above 400 nm,<sup>31</sup> from which we can speculate that adducts **10** and/or **11** would be the carriers of the red-shifted visible absorption band seen in Figure 5. Beyond this speculation, the dimerization reactions giving the azo-derivatives **5** and the hydrogen abstraction leading to the amine **6** are distinct processes and can be surely connected to the changes in the electronic absorption spectra. As concerning the formation of azo-compounds **5**, besides the known bimolecular reactions by which they are formed, namely, the coupling reaction of two triplet nitrenes or the attack of the nitrene triplet to the azide precursor, these compounds can be also produced by the reaction of the arylnitrenium ion with the parent azide.<sup>35</sup>

The ABC photolysis in CHCl<sub>3</sub> may be complicated by the possible formation of adducts of singlet nitrenes with CHCl<sub>3</sub> molecules<sup>36</sup> but they are not spectrally discernible in our study. In the inert CCl<sub>4</sub>, the ABC photooxidation is the main reaction along with dimerization at a lower rate (Fig. 3 (a)).

## CONCLUSION

Photoreactions of ABC bisazide in some fluid media were monitored by UV-Vis spectroscopy and the spectrokinetic analysis have been performed with the help of absorbance and quotient absorbance diagrams, and also of the 3D Mauser space. The spectroscopic behavior describing the photoreactions with 1,2-polybutadiene or poly(methyl methacrylate) put in evidence the instability of the photoproducts. It has been observed the destruction of the azo – derivatives when ABC bisazide was photolysed in the presence of PMMA, and their constant development in the presence of 1,2-PB.

In all studied cases, the photochemistry of ABC follows the generally mechanism of the azide

photolysis, leading to conversion of azide groups into nitro, amino, and azo moieties. This also indicates no special preference for a singlet or triplet state to react from. It can be concluded that, for any of the substrates, the ABC photochemistry is a sum of at least three consecutive photoreactions, partly because some of the photoproducts absorb at the irradiation wavelength. The spectral behavior suggests that, in CHCl<sub>3</sub> and CH<sub>3</sub>OH, ABC undergone photolysis at one single azide group, which has been already observed in other study. This would explain the slower photolysis noted in these solvents and the quite early entry into a photostationary state at a low azide conversion.

## REFERENCES

1. Reiser, F. W. Willets, G. C. Terry, V. Williams and R. Marley, *Trans. Faraday Soc.*, **1968**, *64*, 3265-3575.
2. E. Leyva, M. J. T. Young and M. S. Platz, *J. Am. Chem. Soc.*, **1986**, *108*, 8307-8309.
3. E. Leyva, M. J. T. Young and M. S. Platz, *J. Am. Chem. Soc.*, **1986**, *108*, 3783-3790.
4. Reiser and L. J. Leyshon, *J. Am. Chem. Soc.*, **1971**, *93*, 4051-4052.
5. K. Schrock and G. B. Schuster, *J. Am. Chem. Soc.*, **1984**, *106*, 5228-5234.
6. H. Inui, K. Sawada, S. Oishi, K. Ushida and R. J. McMahon, *J. Am. Chem. Soc.*, **2013**, *135*, 10246-10249.
7. N. Yasuda, S. Yamamoto, Y. Wada and S. Yanagida, *J. Polym. Sci A: Chem.*, **2001**, *39*, 4196-4205.
8. Albini, G. Bettinetti and G. Minoli, *J. Chem. Soc., Perkin Trans.*, **1999**, *2*, 280-28073.
9. S. X. Cai, J. C. Nability, M. N. Wybourne and J. F. W. Keana, *Chem. Mater.*, **1990**, *2*, 631-633.
10. J. Jia and G. L. Baker, *J. Polym. Sci. B: Phys.*, **1998**, *36*, 959-968.
11. M. Avadanei, G. E. Grigoriu and V. Barboiu, *Rev. Roum. Chim.*, **2003**, *48*, 813-819.
12. L. Renaudie, C. le Narvor, E. Lepleux and P. Roger, *Biomacromolecules*, **2007**, *8*, 679-685.
13. H. J. Kim, J. Lee, B. Park, J.-H. Sa, A. Jung, T. Kim, J. Park, W. Hwang and K.-H. Lee, *Kor. J. Chem. Eng.*, **2016**, *33*, 299-304.
14. J. Park, C. Lee, J. Jung, H. Kang, K.-H. Kim, B. Ma and B. J. Kim, *Adv. Funct. Mat.*, **2014**, *24*, 7588-7596.
15. X. Zhang, C. Jiang, M. Cheng, Y. Zhou, X. Zhu, J. Nie, Y. Zhang, Q. An and F. Shi, *Langmuir*, **2012**, *28*, 7096-7100.
16. Y. Yin, X. Lv, H. Tu, S. Xu and H. Zheng, *J. Polym. Res.*, **2010**, *17*, 471-479.
17. E. L. Mishchenko, L. A. Kozhanova, A. Yu. Denisov, N. P. Gritsan, Y. Ya. Markushin, M. V. Serebriakova, T. S. Godovikova, *J. Photochem. Photobiol. B: Biology*, **2000**, *54*, 16-25.
18. K. L. Buchmueller, B. T. Hill, M. S. Platz and K. M. Weeks, *J. Am. Chem. Soc.*, **2003**, *125*, 10850-10861.
19. O. Norberg, L. Deng, M. Yan and O. Ramstrom, *Bioconjugate Chemistry*, **2009**, *20*, 2364-2370.

20. M. Avadanei, submitted.
21. H. Mauser and G. Gauglitz, "Photokinetics. Theoretical Fundamentals and Applications" in "Chemical Kinetics", R. G. Compton and G. Hancock (Eds.), vol. 36, Elsevier Science B.V., Amsterdam, Netherlands, 1998.
22. J. Polster, *Chem. Phys.*, **2001**, 263, 69-81.
23. J. Polster and H. Dithmar, *Phys. Chem. Chem. Phys.*, **2001**, 3, 993-999.
24. P. E. Nielsen and O. Burchardt, *Photochem. Photobiol.*, **1982**, 35, 317-323.
25. E. W. Meijer, S. Nijhuis and F. C. B. M. Von Vroonhoven, *J. Am. Chem. Soc.*, **1988**, 110, 7209-7212.
26. R. A. McClelland, P. A. Davidse and G. Hadzialic, *J. Am. Chem. Soc.*, **1995**, 117, 4173-4174.
27. R. A. McClelland, M. J. Kahley, P. A. Davidse and G. Hadzialic, *J. Am. Chem. Soc.*, **1996**, 118, 4794-4803.
28. P. Ramlall and R. A. McClelland, *J. Chem. Soc. Perkin Trans.*, **1999**, 2, 225-232.
29. P. Ramlall, Y. Li and R. A. McClelland, *J. Chem. Soc. Perkin Trans.*, **1999**, 2, 1601-1607.
30. H. Takeuchi and K. Takano, *J. Chem. Soc. Perkin Trans.*, **1986**, 1, 611-618.
31. V. D. Voskresenska, R. M. Wilson, M. Panov, A. N. Tarnovsky, J. A. Krause, S. Vyas, A. H. Winter and C. M. Hadad, *J. Am. Chem. Soc.*, **2009**, 131, 11535-11547.
32. M. S. Panov, V. D. Voskresenska, M. N. Ryazantsev, A. N. Tarnovsky and R. M. Wilson, *J. Am. Chem. Soc.*, **2013**, 135, 19167-19179.
33. G. B. Anderson, L. L.-N. Yang and D. E. Falvey, *J. Am. Chem. Soc.*, **1993**, 115, 7254-7262.
34. J. C. Fishbein and R. A. McClelland, *J. Chem. Soc., Perkin Trans.*, **1995**, 2, 653-662.
35. J. Xue, Y. Du, X. Guan, Z. Guo and D. L. Phillips, *J. Phys. Chem. A*, **2008**, 112, 11582-11589.
36. S. V. Zelentsov, N. V. Zelentsova and A. A. Shchepalov, *High Energy Chem.*, **2002**, 36, 326-332.